# A Neuro-Synaptic Model of Behavior-Dependent EEG Wave Generation in the Subcortico-Cortical System

**Kenji Itoh**

## Abstract

*A neuro-synaptic model of the subcortico-cortical system was presented on the basis of the interaction among the multiple rhythms of the trains of post-synaptic potentials trains which emerge current source densities or cortical surface potentials. The model was simulated in order to analyze the mechanism for the generation of behavior-dependent electroencephalograms with specific waveforms and spectral patterns, especially hippocampal rhythmic slow activity, as well as large amplitude, irregular slow activity. The simulated electroencephalograms showed rhythmic as well as irregular waves with frequency fluctuation.*

## Introduction

A number of studies on brain rhythm as a candidate for the command of neural timing in human behavior have appeared, including serial order in behavior incorporated in interactional as well as internal synchrony[1]. The fundamental rate of such synchronous timing for performance and perceptual behavior is said to be from 5 to 10Hz, including 7Hz in stuttering, 5Hz in monotone, etc.[2]

Electroencephalograms (EEGs), magnetoencephalograms (MEGs) also show a rhythmic pattern, and can produce information on neural timings if they reflect cortical activities[3]. EEGs/EMGs consist of several basic rhythms, including the infra-slow wave( <1Hz), the delta wave (1-3Hz), theta wave(3-7Hz), alpha wave (7-14Hz), beta wave (14-28Hz) and the gamma wave (>20Hz)[4].

Changes in internal and external states influence EEGs. During sleep, the delta component is most prominent. During quiet wakefulness with eyes-closed, however, the prominent component is the alpha wave, the frequency of which correlates with brain size[5]. Vanderwolf observed the hippocampal activity during wakefulness in a rat which showed a rhythmical slow activity (RSA) in type 1 behavior (including walking, swimming, rearing and digging), as well as large amplitude irregular activity (LIA) in type 2 behavior (including alert immobility, teeth chattering, sneezing and vocalization). Cortical rhythms have been reported as having a correlation with behavioral timing[6].

Recent applications of multielectrodes to the cortex have made it possible to obtain "micro-EEGs" which can obtain information on cortical activities, i.e., micro-EEGs intermediate between a single neuron firing and macro-EEGs. Micro-EEGs are related to current source densities (CSDs) which are generated by the action potentials of neurons as well as by synaptic potentials, but only CSDs from excitatory potentials are observed at the cortical surface as monopolar potentials. These surface potentials may be positive or negative according to the direction and number of pairs of CSD sources and sinks[7].

Based on these physiological data, various models of brain rhythmicity have been proposed, such as a local neural circuit with or without reccurent inhibition in the thalamus or in the cortex, a global standing wave in the cortex and a thalamic chemical clock[8].

In the present paper, a neuro-synaptic model of the subcortico-cortical system will be presented on the basis of the interaction of a few trains of positive and negative cortical surface potentials generated by CSDs originating from excitatory postsynaptic potentials (EPSPs) in order to analyze the mechanism of the formation of cortical rhythms with behavior-dependent waveforms as well as spectral patterns[9].

## The Model

In this model, the process of rhythmic wave formation is performed as follows.

1) Scalp EEGs are assumed to be near field surface potentials derived from CSDs analogous to the EPSPs.
2) The periodic oscillations are generated in the subcortical systems, i.e., the thalamic complex of the specific and nonspecific nuclei, the nucleus basalis, the medial septum-diagonal band of Broca, and the brain stem reticular formation.
3) The oscillator nuclei, some of which are mutually connected, project periodic bursts at different layers in the cortex.
4) A burst in each layer generates EPSPs with an intensity proportional to the burst density.
5) The CSDs from the EPSPs evoke positive or negative cortical surface potentials according to the level of the layer of the CSD source and sink.
6) The subcortical process of rhythmic burst generation is modulated directly or indirectly through the other subcortical generators, including the nucleus basalis as well as the brainstem reticular formation.
7) The multiple trains of isolated events which emerge from the above processes are superimposed to form a "cortical EEG rhythm".

The EPSP can be modeled by an equivalent circuit composed of a resting membrane potential (E), resistance (1/G), capacitance (C) and shunt conductance (mg) as shown in Fig. 1. During a membrane conductance change, the EPSP, v(t), is described by the following.

$$dv/dt + (G + mg)v/C - mg.E/C = 0 \qquad (1)$$

After conductance change ceases,

$$dv/dt + G/C = 0 \qquad (2)$$

Using an approximation of the conductance change with a composite curve of the cosine and sine waves, the time course unit for the EPSPs, V(t), is simplified as follows,

$$V(t) = \begin{cases} [1 - \cos(t/T_c)]/2 & (0 <= t < T_c) \\ \exp[ - (t - T_c)/T_d] & (T_c = t) \end{cases} \quad (3)$$

where $T_c$ is the duration of the conductance change, and $T_d$ is the discharging time constant. When the EPSP is generated repetitively, the EPSP is as follows.

$$V(t) = \begin{cases} [1 - \cos(t/T_c)]/2 & (0 <= t < T_c) \\ [\exp( - (t - T_c)/T_d) - V_o]/(1 - V_o) & (T_c <= t < T) \end{cases} \quad (4)$$

$$V_o = \exp[ - (T - T_c)/T_d] \quad (5)$$

$$V(t + T) = V(t) \quad (6)$$

where T is the period of the repetitive stimuli[10]. The cortical surface potentials are specified by the layer of the generated EPSPs as in Fig. 2. If the surface potential, Vi(t), is generated by the EPSPs in the i-th cortical layer, the summated surface potential, S(t), is as follows.

In the case where the amplitude of Vi(t) is modulated by the wave function Mi(t), the summated surface potential, S(t), is

$$S(t) = \sum_{i=1}^{n} a_i, B(1 + m_i, M_i(t)), V_i(t - d_i) \quad (7)$$

$$B(x) = \begin{cases} B(x) & (B(x) >= 0) \\ 0 & (B(x) < 0) \end{cases} \quad (8)$$

where $a_i$ and $d_i$ are the amplitude and delay of $V_i$, respectively; n is the number of cortical layers; $m_i$ is the modulation depth; and B(x) is a half-wave rectifier.

The neural clock generator can be simplified by a relaxation oscillator[11]. One burst cycle, $T_i$ of each $V_i(t)$is composed of a burst of spikes and a silent period, in which an inactivation upon depolarization occurs due to the transmembrane flux of calcium through a voltage-dependent channel activated by the neuronal membrane depolarization. If the burst interval is T, the burst and silent periods are $T_b$ and $T_s$, as follows.

$$T = T_b + T_s \quad (9)$$

The model system, as given in Fig. 2, consists of a set of five neuronal assemblies layered in the subcortico-cortical system, i.e., a cortex with several layers (CX), cortical inputs from the subcortical nuclei or other cortical areas ($S_1$, ..., $S_n$), the nucleus basalis (NB) and the midbrain reticular formation (RF).

The inputs $S_i$ are projected to the deep and surface layers in the cortex, respectively. The activity of $S_i$ is modulated in amplitude as well as in repetitive frequency by the slow cholinergic RF directly or indirectly through NB, which also projects its output to the CX.

## Simulation and Results

The model was used to simulate rhythmic waves using the unit EPSP with $T_c/T$ = 1/3 and $T_d/T$ = 2/3.

Figure 3a shows the simulated rhythmic waves obtained with only two surface potentials with the same amplitudes but reversed polarity ($a_2 = -a_1$, $d_2 - d_1 = 0$) from the respective deep and surface layers at various ratios of repetitive frequencies ($T_1/T_2$ = 10/5 to 10/15), but with no amplitude modulation by the RF. The model could simulate the waxing and waning pattern of a rhythmic wave except at the ratio of 10/10. Also as in Fig. 3b with a phase shift ($d_2 - d_1 = T_1/2$), shows a pseudo-sinusoidal wave at the ratio of 10/10.

Figure 4a shows the simulated rhythmic waves obtained with the same surface potentials as in Fig.3, but without reversed polarity. The model system could simulate rhythmic waves with frequency fluctuations as well as waxing waning. In the case of a phase shift, Fig. 4b, the rhythmic wave shows a pseudo-sinusoidal wave at the ratio of 10/10, but with half the period of that in Fig. 3b.

Figure 5 shows the result from the superimposed surface potentials of two summated surface potentials composed of two surface potentials with the same amplitude and period, but polarity reversed, and some delay ($d_2 - d_1 = T_1/3$, $d_4 - d_3 = T_3/3$).

Figure 6 shows the power spectra of the summated surface potentials shown in Fig. 4, 5 and 6. In the case of the ratio of 10/8, there are line spectra at the fundamental frequency of each repetition, as well as decreasing harmonics in the higher orders, but at the ratio of 10/10 with phase shift, only the fundamental component is prominent.

## Discussion

A neuro-synaptic model of EEG generation was presented without using sinusoidal waves, but using instead distorted saw-tooth-like waves with harmonics analogous to postsynaptic potentials as basic units. Rhythmic EEGs could be simulated based on two simple interactions among a restricted number of such basic units, i.e. linear summations, and amplitude modulation.

The model system with two summated surface potentials linearly superimposed could simulate the generation of a sinusoid-like wave at the fundamental as well as at the second harmonic frequency, with no use of a nonlinear function, as shown in Figs. 4b and 5b. The thalamic neurons is said to show firing patterns in two frequencies, 6 and 10 Hz[12]. It is now difficult to determine the respective modes for the generation of such rhythmic waves among theta[13], alpha and beta bands[14].

The rhythmic frequency is determined fundamentally by the metabolic rate. Some fluctuations in such fundamental frequencies can occur by changing the metabolic rate directly or indirectly through inhibitory innervation. The hippocampal LIA shows rapid fluctuations in amplitude as well as in frequency. In the present model such LIA-like waves, as well as RSA-like waves, could be generated by a linear summation of only two simple rhythmic waves with steady amplitude and frequency, and without complex nonlinear oscillators[15].

There are many neuro-synaptic circuits showing temporal rhythmic activities within the brain. e.g., the thalamo-cortical system[16], the septo-hippocampal system[17] and the striato-motor system[18], all of which consist of cortical layers and multiple inputs at different levels. Our model can be applied to such rhythmic system for the further analysis of the rhythmic waves relating to human behavior[19], and the interaction among these multiple generators with different rhythmic patterns must be incorporated into the model[20].

*Acknowledgements*----The valuable suggestions of S. Niwa, K. Hiramatsu, M. Fukuda, O. Saitoh, K. Nakagome, A. Iwanami, T. Sasaki, H. Honda and S. Hayashida.

**References**

1) Meek J (1992) Why run parallel fibers parallel Teleostean Purkinje cells as possible coincidence detectors, in a timing device subserving spatial coding of temporal differences. Neurosci 48, 249-283.
2) Waibel A (1986) Suprasegmentals in very large vocabulary word recognition. In Schwab EC, Nasbaum HC (eds) Pattern recognition by humans and machines, vol.1, speech perception, Academic Press: Orland, FL, 159-186.
3) Funke K, Eysel UT (1992) EEG-dependent modulation of response dynamics of cat dLGN relay cells and the contribution of corticogeniculate feedback. Brain Res 573, 217-227.
4) Riekkinen P, Buzsaki G, Riekkinen PJr, Soininen H, Partanen J (1991) The cholinergic system and EEG slow waves. Electroenceph Clin Neurophysiol 78, 89-96.
5) Llinas R (1990) Intrinsic electrical properties of nerve cells and their role in network oscillation. In Cold Spring Harbor symposia on quantitative biology, vol. LV, the Brain, Cold Spring Harbor Laboratory Press: New York, 933-938.
6) Vanderwolf CH (1992) The electrocorticogram in relation to physiology and behavior: a new analysis. Electroenceph Clin Neurophysiol 82, 165-175.
7) Mizdorf U (1991) Physiological sources of evoked potentials. Electroenceph Clin Neurophysiol, Suppl 42, 47-57.

8) Dossi RC, Nunez A, Steriade M (1992) Electrophysiology of a slow (0.5-4Hz) intrinsic oscillation of cat thalamocortical neurones in vivo. J Physiol 447, 215-234.
9) Itoh K (1991) A neuro-synaptic model of state-dependent EEG waves in subcortico-cortical system. Med Biol Eng Comput 29(S), 486.
10) Itoh K (1991) A neuro-synaptic model of state-dependent EEG wave generation in the subcortico-cortical system. Ann Bull RILP, Univ Tokyo 25, 221-241.
11) Linkens DA (1979) Biological systems, modelling and control, Peter Peregrinus: Stevenage.
12) Nunez A, Dossi RC, Contreras D, Steriade M (1992) Intracellular evidence for incompatibility between spindle and delta oscillations in thalamocortical neurons of cat. Neurosci 48, 75-85.
13) Konopacki J, Bland BH, Roth SH (1988) Carbachol-induced EEG 'theta' in hippocampal formation slices: evidence for a third generator of theta in CA3c area. Brain Res 451, 33-42.
14) Kuhlman WN (1980) The mu rhythm: functional topography and neural origin. In Pfurtscheller G., Buser P., Lopes da Silva F. H., Petsche H. (eds.) Rhythmic EEG activities and cortical functioning. Elsevier: North-Holland. 105-120.
15) Sclabassi RJ, Eriksson JL, Port RL, Robinson GB, Berger TW (1988) Nonlinear systems analysis of the hippocampal perforant path-dentate projection. I. Theoretical and interpretational considerations. J Neurophysiol 60, 1066-1076.
16) Crunelli V, Leresche N (1991) A role of GABAb receptors in excitation and inhibition of thalamocortical system. Trends Neurosci 14, 16-21.
17) Stewart M, Fox SE (1989) Two populations of rhythmically bursting neurons in rat medial septum are revealed by atropine. J Neurophysiol 61, 982-993.
18) Lorenzon NM, Foehring RC (1992) Relationship between repetitive firing and afterhyperpolarizations in human neocortical neurons. J Neurophysiol 67, 350-363.
19) Cao F, Leung LS (1991) Behavior-dependent paired-pulse responses in the hippocampal CA1 region. Exp Brain Res 87, 553-561.
20) Doty RW (1990) Time and memory. In McGaugh JL, Weinberger NM, Lynch G (eds) Brain organization and memory: cells, systems and circuits, Oxford Univ Press: New York, 145-158.

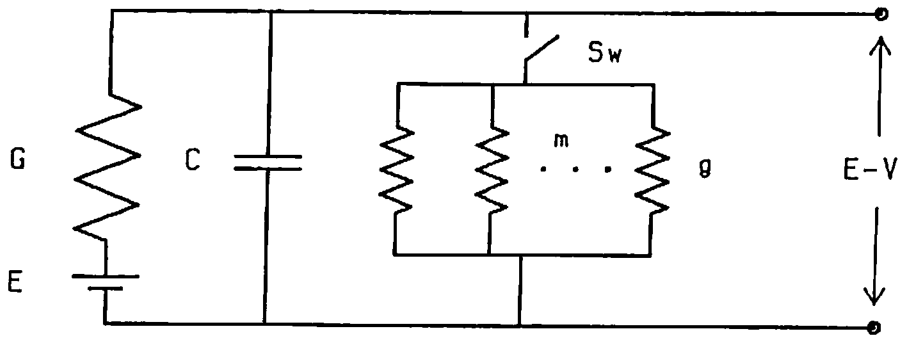


Fig. 1 Electrical circuit model of the postsynaptic membrane. C: membrane capacitance; E: resting membrane conductance; m: number of quanta transmitted by one pulse; Sw: switch of ion channel; V: postsynaptic potential

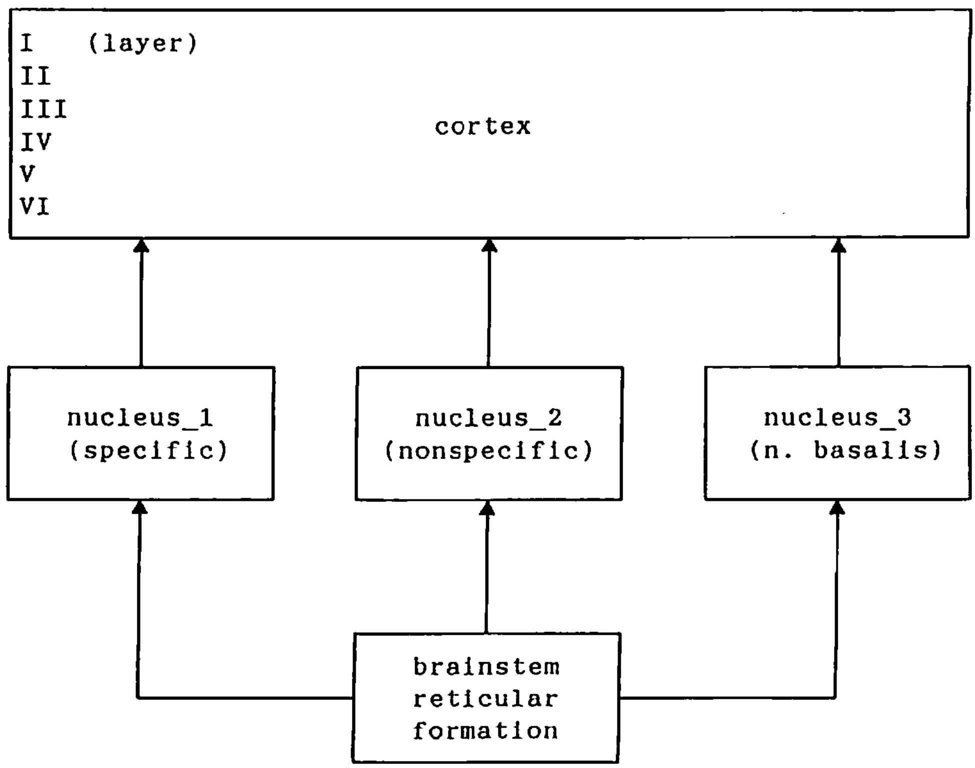


Fig. 2 Block diagram of the subcortico-cortical system

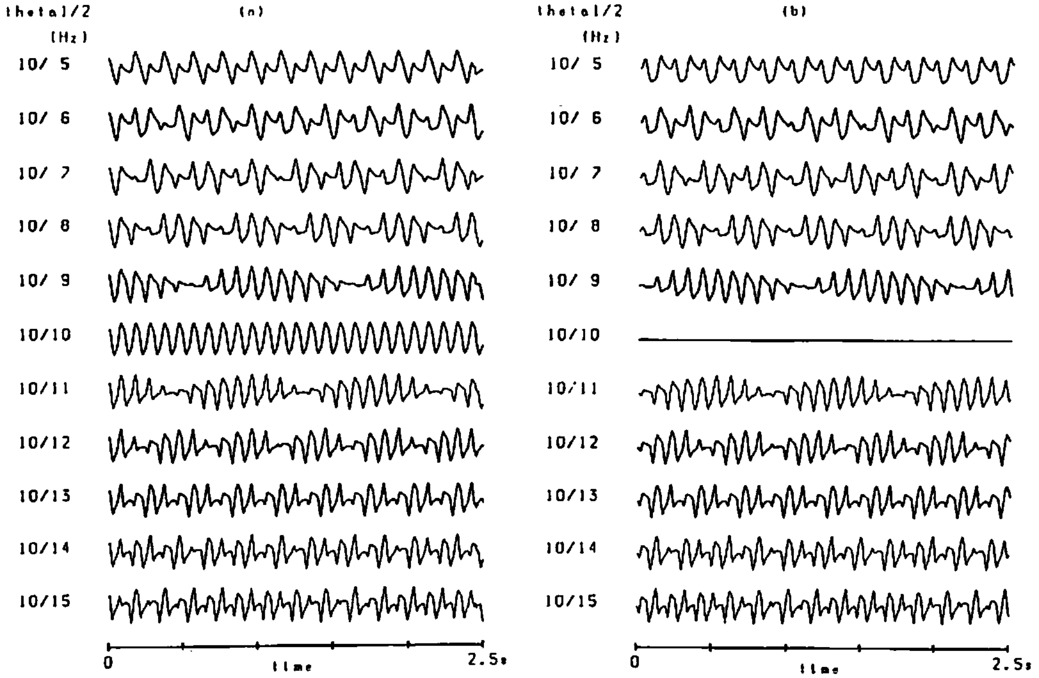


Fig. 3 Rhythmic response of the system with the PSP charging duration $T_c$ = T/3 (T: period of burst train) and discharging time constant $T_d = 2T_c$. Theta 1/2: frequency ratio $T_1/T_2$ of the first surface potential (positive) and second potential (negative) ($a_2 = -a_1$). (a): $d_2 - d_1 = 0$; (b): $d_2 - d_1 = T_1/2$

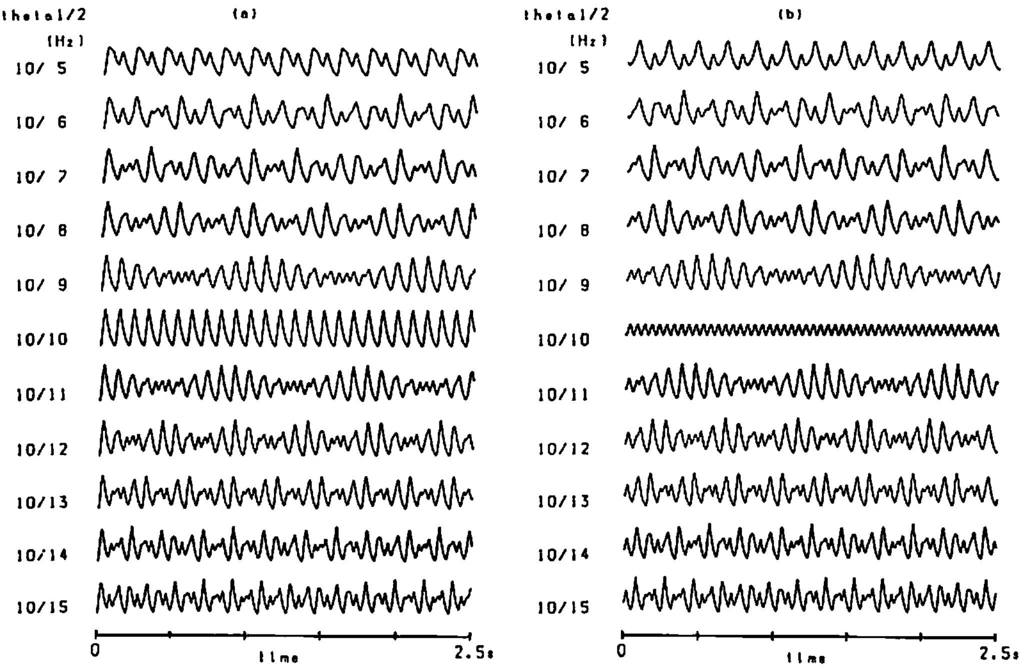


Fig. 4 The same as in Fig. 3 but with $a_2 = a_1$

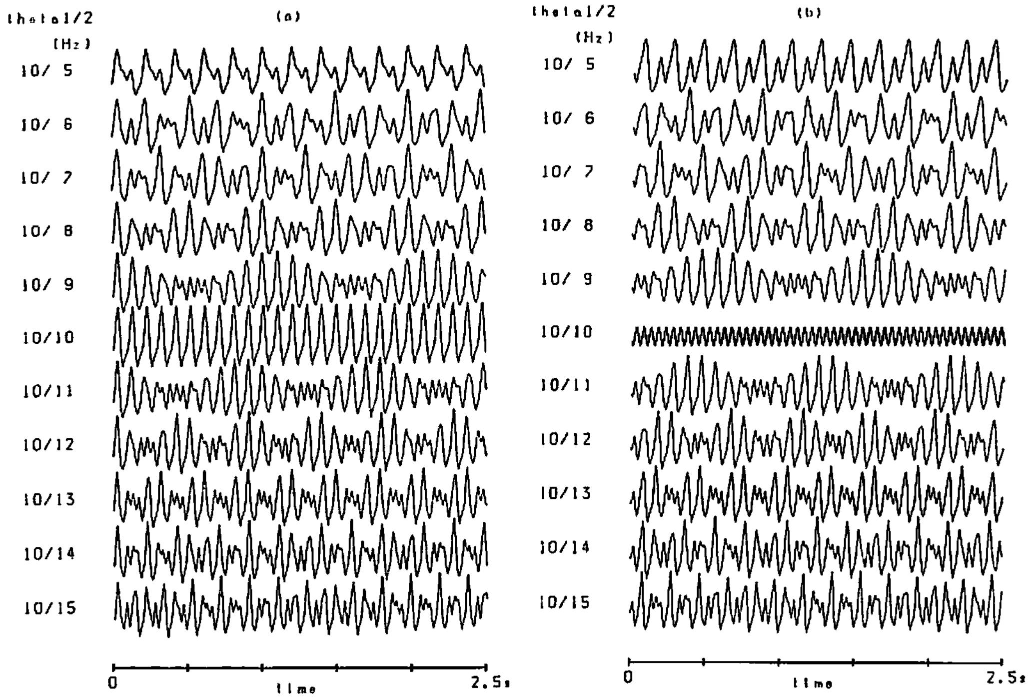


Fig. 5 Rhythmic response of the system with two summated potentials from two surface potentials having the same amplitude and frequency but polarity reversed ($a_2 = -a_1$, $a_4 = -a_3$) and delay ($d_2 - d_1 = T_1/3$, $d_4 - d_3 = T_3/3$)

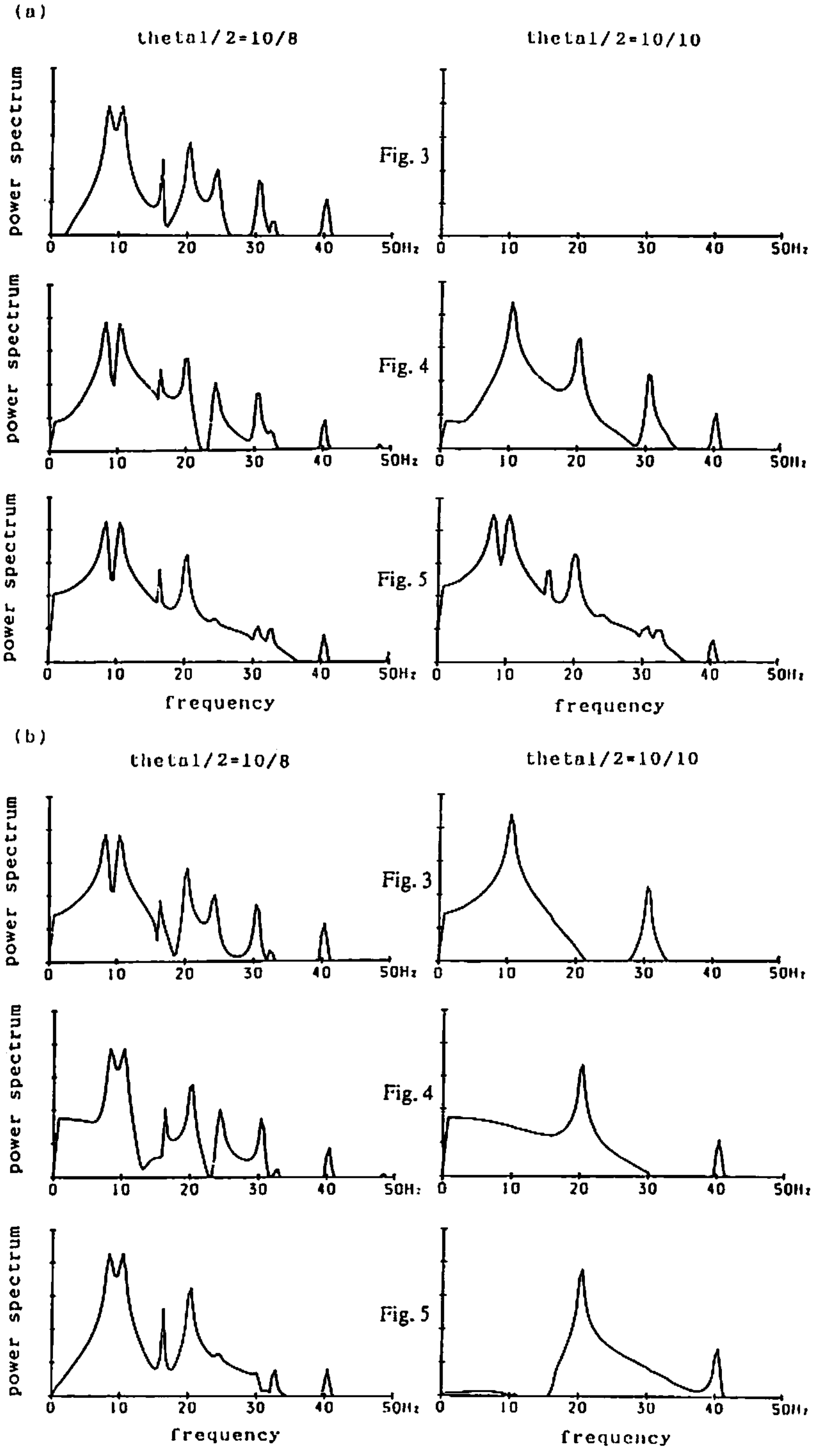


Fig. 6 Examples of power spectra of the summated surface potentials shown in Fig. 3, 4, and 5. (a): $d_2 - d_1 = 0$; (b): $d_2 - d_1 = T_1/2$